Biotechnology and Bioengineering

WILEY

BIOTECHNOLOGY AND BIOENGINEERING

ARTICLE

AB-Panda: An AI-Generated Antibody Structure-Based Tool for Developability Prediction

Wu Zou[1] | Jianjun Deng[2] | Yun Shen[2] | Tao Zhang[1] | Zhitong Bing[3] | Lingyan Yuan[4] | Chen Huang[2] | Jianghai Liu[1,2,5] | Xin Lei Li[1,5]

[1]School of Bioscience and Technology, Chengdu Medical College, Chengdu, Sichuan Province, China | [2]ABLINK Biotech Co. Ltd, Chengdu, Sichuan Province, China | [3]Institute of Modern Physics, Chinese Academy of Sciences, Lanzhou, Gansu Province, China | [4]Advanced Energy Science and Technology Guangdong Laboratory, Huizhou, Guangdong Province, China | [5]Sichuan Higher Education Institute Key Laboratory of Major Disease Target Discovery and Protein Drug Development, Chengdu Medical College, Chengdu, Sichuan Province, China

Correspondence: Jianghai Liu (jianghai.liu@cmc.edu.cn) | Xin Lei Li (xinlei.li@cmc.edu.cn)

Received: 1 July 2025 | **Revised:** 22 September 2025 | **Accepted:** 11 October 2025

Keywords: computation tool | developability prediction | unit-area hydrophobic value | unit-area negative charge | unit-area positive charge

ABSTRACT

The developability of antibodies is a critical concern in antibody discovery, encompassing issues such as self-interaction, aggregation, and thermal stability. The use of computational and structure-based tools has greatly improved the evaluation and prioritization of initial antibody sequences. With the increasing demand for subcutaneous administration of small-volume, high-concentration antibody formulations, there is a need for more accurate prediction tools based on protein structures. Our study introduces AB-Panda, a tool based on AlphaFold2-predicted antibody structures and three innovative structure-related metrics. AB-Panda utilizes unit-area hydrophobic value (UHV), unit-area positive charge (UPC), and unit-area negative charge (UNC) to automatically identify hydrophobic and charged patches within the complementarity determining regions (CDRs) of antibodies. Through the analysis of the 919 clinical stage therapeutic (CST) antibodies, we have established recommended ranges of UHV, UPC, and UNC as reference standards for antibody developability. AB-Panda offers clear visualizations of surface hydrophobic and charge distribution, facilitating the identification of problematic amino acids and providing suggestions for further sequence engineering. Additionally, AB-Panda has been integrated into a web application, available at https://www.antibodydev.com, by combining UHV, UPC, UNC, and other established computational metrics for the early screening and optimization of antibody sequences.

1 | Introduction

The presence of over 1000 antibody therapies in clinical trials marks the advent of the precision treatment era. Antibody drugs have become important tools in treating cancer, inflammatory diseases, and autoimmune diseases due to their high specificity and low side effects (Pleguezuelo et al. 2021; Fugger et al. 2020). Despite the enormous potential of antibody drugs in treating various complex diseases, the high costs, the long development cycles, and the high failure rate, remain major obstacles to their widespread application (Fazenda et al. 2013; Calvo and Zuniga 2012). It is estimated that the average cost of developing a new drug is approximately $2.6 billion with the process typically taking 10 to 15 years (Sripriya Akondi et al. 2022; DiMasi et al. 2016). Moreover, approximately 99% of drug candidates will fail to win approval (Fogel 2018).

The development of antibody drugs face challenges across multiple domains, including pharmaceutical attributes such as stability, viscosity, manufacturability, as well as clinical performance factors such as bioavailability and the choice between subcutaneous (S.C.) and intravenous (I.V.) administration

(Jiskoot et al. 2022). Recently engineered antibody formats, like smaller fragments and bispecific antibodies, are attracting increased interest, but they are characterized by higher instability than conventional antibodies, particularly in terms of aggregation (Condado-Morales et al. 2024). Additionally, for some chronic diseases, subcutaneous administration of high-concentration antibody formulations is favored, despite facing solubility challenges at high concentrations (Li et al. 2019). Therefore, many antibodies fail drug development due to low solubility, aggregation or poor pharmacokinetics. These failures have prompted innovative approaches, including artificial intelligence-based protein structures and high-throughput screening technologies to predict developability, reducing the risk of failure during clinical trials (Condado-Morales et al. 2024; Bailly et al. 2020; Chen et al. 2024; Yamankurt et al. 2019).

Therapeutic antibody profiler (TAP) provides five developability guidelines based on complementarity determining region (CDR) length, CDR patches of surface hydrophobicity, CDR patches of negative charge, and structural Fv charge symmetry parameters (Raybould et al. 2019, 2024). These and other studies highlight surface hydrophobicity and charge distribution as crucial factors shaping antibody physicochemical properties, influencing solubility, stability in aqueous solutions, and interactions with other biomolecules and themselves (Song et al. 2021; Hebditch and Warwicker 2019; Hladílková et al. 2016). In TAP, surface hydrophobicity and charge (positive and negative) are evaluated across the entire protein, making it difficult to pinpoint specific amino acids or regions with unfavorable properties when poor scores or developability issues arise. To address this, we introduce AB-Panda, a novel tool that tackles this challenge with three innovative metrics: unit-area hydrophobic value (UHV), unit-area positive charge (UPC), and unit-area negative charge (UNC) of antibodies' CDR regions. The Unit-area method intuitively quantifies the hydrophobic intensity and charge density in local regions by averaging hydrophobic values (UHV) and charge values (UPC/UNC) over the solvent-accessible surface area (SASA) of each surface-exposed residue. AB-Panda integrates Alphafold2 to automatically generate 3D structure models of antibodies, and then calculates and highlights UHV, UPC and UNC values for each of the six CDR regions. By analyzed UHV, UPC and UNC scores from 919 clinical-stage antibody therapeutics (CSTs), we established recommended ranges for these metrics to predict antibody developability. Last, we do systematic comparisons of AB-Panda and TAP based on experimentally measured biophysical properties of antibodies, suggesting AB-Panda's superior performance in identifying developability-challenged antibodies. This analytical approach not only aids in revealing the developability characteristics of antibodies at the sequence and structural levels but also lays a solid foundation for functional evaluations and sequence optimization.

2 | Methods

2.1 | Algorithm Workflow

The CDR regions of antibodies were defined according to IMGT numbering. In addition, for specific details of IMGT—such as the definition criteria for CDR regions—reference can be made to the work "AbNumber" published by GitHub author Prihoda (Tags: v0.4.0). Antibody structures were generated using AlphaFold2, which enables a high-precision three-dimensional (3D) structure predictions even in the absence of experimental structural data. All of our protein structural models were generated using AlphaFold2.30. The process was run on our custom-built ABLINK BioAI for Scientists computational platform with the following settings: max_template_hits = 20, relax_max_iterations = 0, model_type: str, r --use_gpu_relax = true, models_to_relax = all, db_preset = full_dbs, benchmark = false, model_preset = monomer. For each modeling run, five structures were ranked using the local-distance difference test (plDDT), and the top-ranking protein prediction model was used for further structural analysis.

2.2 | Formulas Used

Based on the AI-generated antibody structures, the number of the exposed residues were identified using equation (1), and the UHV, UPC, and UNC were calculated using equations (2) and (3).

$$[A_{actual}/A_{Max} \geq 7.5\%]. \quad (1)$$

$$UHV = \frac{\sum X_i}{A_{CDR}}. \quad (2)$$

$$UPC/UNC = \frac{\sum q_i}{A_{CDR}}. \quad (3)$$

A_{actual} is the actual solvent accessible surface area (SASA) of each amino acid calculated using Biopython's DSSP(Dictionary of secondary structure of proteins) module (Cock et al. 2009). A_{max} is the maximum SASA of each amino acid referential form Matthew Z. Tien (Tien et al. 2013). i is the number of amino acids in the exposed state. X_i is based on the hydropathy score for residue R in Eisenberg D. scale (Eisenberg et al. 1984). A_{CDR} is the total relative SASA for exposed residues in the CDR region. q_i is the charge of the surface-exposed residues and the charges is assigned by sequence as follows: ASP: −1, GLU: −1, LYS: +1, ARG: +1, HIS: +0.1.

2.3 | Data Processing

All CST sequences were processed and the three UHV, UPC, and UNC metrics were calculated using the above formulas (Supporting Information Table S1). For data analysis, we initially extract the specified data columns and apply the inter quartile range (IQR) method to remove outliers, thereby maintaining data stability and consistency. Removing extreme values helps reduce the influence of random factors and measurement errors on the results, ensuring that statistical metrics such as mean and standard deviation more accurately reflect the true distribution and avoid misleading deviations. We then acquired basic statistics (e.g., maximum, minimum, mean, standard deviation, and sample size) for the filtered data, which serves as the basis for determining the prediction interval. At an 85% confidence level, we use the critical value of the t-distribution, the sample standard deviation, and the mean to establish the upper and lower bounds

of the prediction interval, yielding a recommended range. This range is primarily intended to achieve stability and reliability in the analysis process.

2.4 | Result Presentation

After generating the 3D structure of the antibody, AB-Panda incorporates UHV, UPC, and UNC as key metrics to reflect the local surface hydrophobicity and charge distribution within the CDR regions. These metrics are marked with varying intensities of color in the 3D structure of the antibody, providing an intuitive visualization of hydrophobic clustering and charge effects. In our AB-Panda tool, when we input the VH sequence and VL sequence of an antibody, to ensure the accuracy and stability of structure prediction, our algorithm will insert a 15-amino-acid Linker (GGGGSGGGGSGGGGS) between VH and VL. This Linker is used to connect VH and VL, forming a structure similar to single-chain variable fragments (scFvs). As shown in Figure 2 and Figure 5, it features a long-region Linker structure.

3 | Results

3.1 | Protein Surface Hydrophobicity Calculated By AB-Panda

Hydrophobicity in the CDR regions of mAbs has been consistently linked to aggregation propensity (Raybould et al. 2019). We adopted the unit-area Hydrophobic Value (UHV) as the evaluation metric of the CDR hydrophobicity, considering only surface-exposed amino acids which have a side chain with relative accessible surface area [$A_{actual}/A_{max} \geq 7.5\%$] (Raybould et al. 2019). After summarizing the UHV value of the six CDRs from the 919 CSTs, the 85% prediction interval for these UHV were depicted as blue bars in Figure 1, representing the recommended range of UHV. The figure clearly shows that UHV within the recommended range are relatively uniformly distributed across different CDR regions, providing a concrete and actionable reference for antibody optimization. Most UHVs are concentrated within the recommended range H1(−20.3755 ~ 67.7765), H2(−72.5943~58.5736), H3(−98.2091~48.7332), L1(−86.6160~12.8772), L2(−140.1522~96.4115), L3(−79.4906 ~ 83.9895) indicated by the densely populated blue bars (Figure 1). Samples with UHV that significantly deviate from the recommended range are fewer. UHV below the recommended range may indicate insufficient hydrophobicity, potentially affecting antibody stability or reducing developability (Geller et al. 2018a), whereas UHV above the recommended range may be associated with excessive hydrophobicity, which could increase the risk of aggregation or solubility issues under high concentration conditions (Wang et al. 2010).

We tested AB-Panda using antibodies with experimentally defined hydrophobicity levels. Tusha previously evaluated 137 advanced clinical-stage antibodies across various biophysical property assays (Jain 2017a). From these, three assays measuring hydrophobicity were selected: hydrophobic interaction chromatography (HIC), standup monolayer adsorption chromatography (SMAC), and salt-gradient affinity-capture self-interaction nanoparticle spectroscopy (SGAC-SINS) (Jain 2017a). Since higher values in these assays indicate greater hydrophobicity, the top two antibodies, lirilumab and glembatumumab, were chosen for AB-Panda's evaluation (Supporting Information Table S2). AB-Panda's analysis showed that the UHV value of the lirilumab

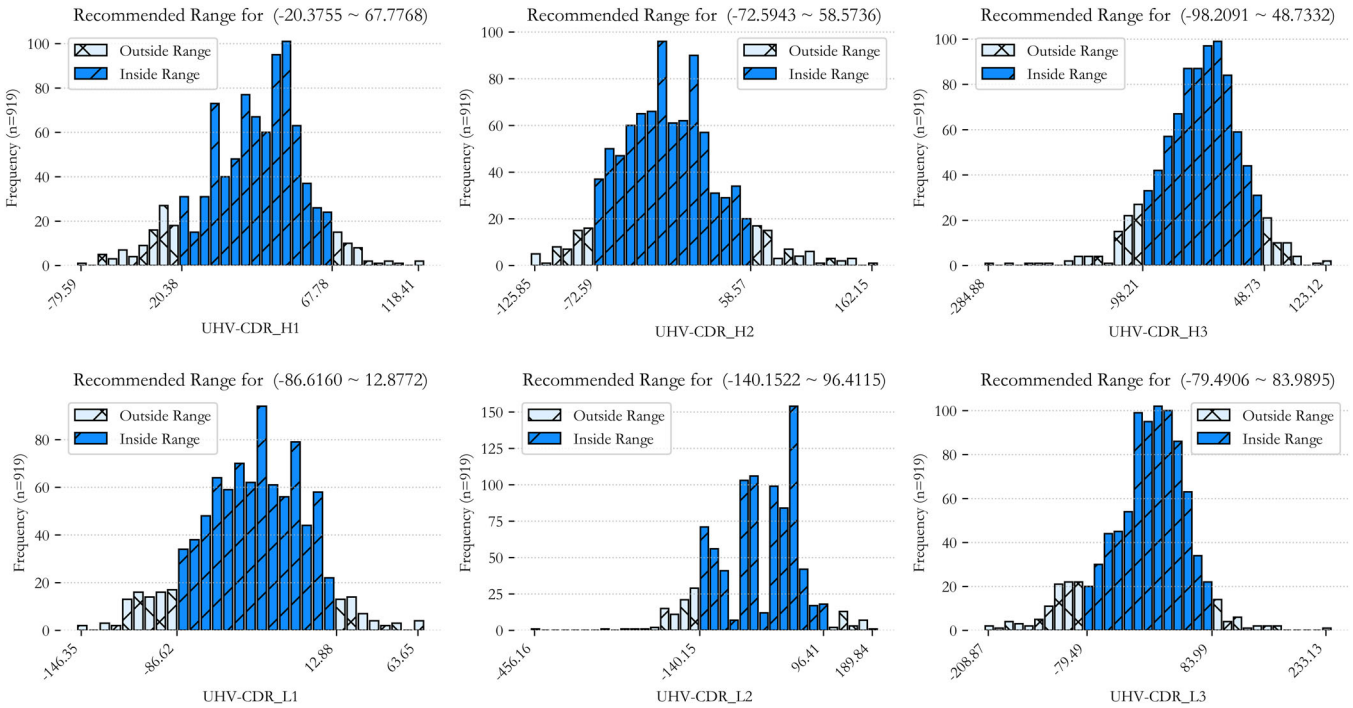

FIGURE 1 | The recommended range of UHV was constructed using 919 CST sequences. The figure includes six subplots, each representing a different CDR region (H1, H2, H3, L1, L2, L3). In each subplot, blue bars indicate the distribution of samples with UHV within the recommended range, while gray bars represent samples with UHV outside the recommended range.

CDR-H2 was 168.03 and the UHV value of the glembatumumab UHV CDR-L1 was −107.43, both of which significantly exceeds our recommended range. The UHV distribution across lirilumab's CDRs, as calculated by AB-Panda, is illustrated in Figure 2. Notably, despite these outlier values, their hydrophobic CDR patches remained within the permissible range predicted by TAP. To evaluate the potential structural impact of inserting the 3xG4S linker on antibodies, we employed molecular docking and molecular dynamics (MD) simulations. We selected lirilumab—the exemplary antibody in the manuscript—and its target, killer-cell immunoglobulin-like receptors (KIR). The docking results identified multiple sets of residues between the antibody and target contributing to hydrogen bond formation. Following the docking analysis, MD simulations were conducted, and the results demonstrated favorable outcomes. Comprehensive details of the docking and MD stimulation results are provided in the Supplementary Files (Figures S1–S6 and Table S5). Based on these findings, we conclude that the insertion of the linker mimics the native antibody structure and does not disrupt antibody and antigen binding. Furthermore, we considered whether the presence of the linker would affect antibody structural stability. We used Rosetta energy calculation tool to compare the stability of the antibody with and without the linker. The calculated energy for the antibody with the linker was −1077.110, while that for the antibody without the linker was −1072.574. Since a lower energy value indicates higher protein stability, these results suggest that inserting the 3xG4S linker does not compromise the stability of the antibody.

3.2 | Protein Surface Charge Calculated by AB-Panda

Surface charge patches have been linked to unfavorable viscosity at high concentrations and rapid pharmacokinetic (PK) clearance (Raybould et al. 2019; Thorsteinson et al. 2021). These patches are integrated as developability predictors in tools like TAP, which evaluates charge distribution across the six CDR regions using the patches of positive charge (PPC) and the patches of negative charge (PNC) (Raybould et al. 2019; Thorsteinson et al. 2021). AB-Panda enhances this approach by introducing UPC and UNC values, enabling precise localization of problematic regions and specific amino acids within the CDRs. Analysis of UPC and UNC scores across 919 CST

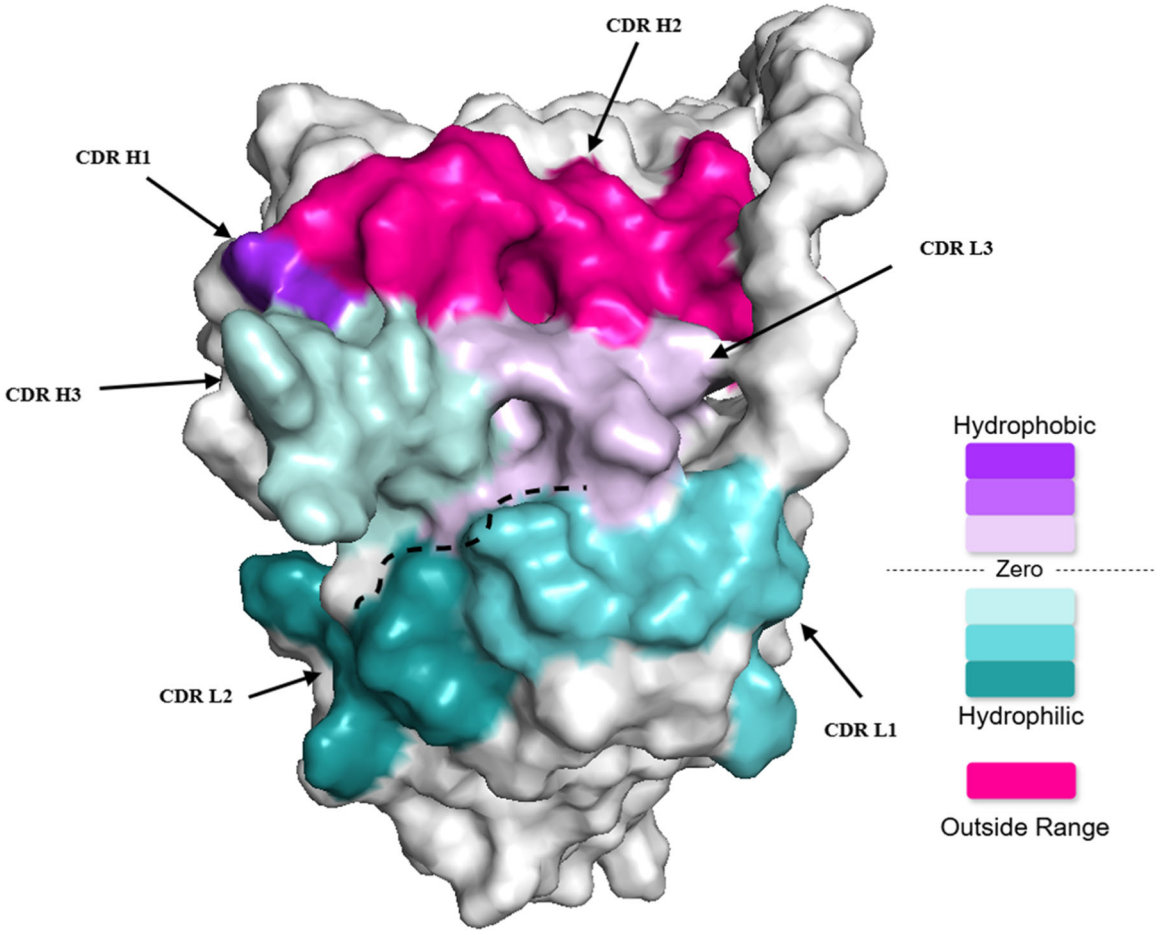

FIGURE 2 | The distribution of UHV across the CDRs of the antibody lirilumab. The UHV values of lirilumab are 68.89, 168.03, and −21.46 for CDRH1-H3, and −31.52, −109.07, and 18.78 for CDRL1-L3. The color scale in the lower-right corner indicates the gradient of UHV values from hydrophilic (negative values) to hydrophobic (positive values), with zero as the dividing line. Positive UHV values above zero signify increasing hydrophobicity, represented by progressively darker shades of violet, whereas negative UHV values below zero indicate greater hydrophilicity, depicted by increasingly darker hues of blue. Areas highlighted in hotpink denote regions that fall outside the recommended range for UHV and thus warrant consideration for mutational optimization.

antibodies highlights the charge distribution trends within CDR regions in this antibody library (Figure 3). We established the recommended range as UPC H1(279.14~391.33), H2(237.54 ~ 341.44), H3(240.95~454.17), L1(252.26~358.52), L2(311.88 ~ 522.24), L3(300.91~514.96) and UNC H1(−403.26 ~ −276.59), H2(−356.96 ~ −240.92), H3(−454.92 ~ −251.79), L1(−370.69~ −188.70), L2(−595.53 ~ −273.39), L3(−524.01 ~ −303.55).

Charge descriptors have demonstrated utility in predicting high-concentration viscosity and, in some cases, aggregation propensity. Two key assays, Affinity-Capture Self-Interaction Nanoparticle Spectroscopy (AC-SINS) and Clone Self-Interaction by Bio-Layer Interferometry (CSI), are essential for evaluating antibody self-interactions. High AC-SINS or CSI values, indicating strong self-interactions, are often associated with increased viscosity at therapeutic concentrations, presenting significant formulation challenges (Jain 2017a; Liu et al. 2005). To evaluate the predictive performance of UPC and UNC metrics on published data (Jain 2017a), the antibodies glembatumumab and duligotuzumab with exceptionally high AC-SINS or CSI values were analyzed using AB-Panda. Aligned with biophysical data, AB-Panda identified both antibodies as problematic, confirming its effectiveness in detecting potential developability risks (Supporting Information Table S2).

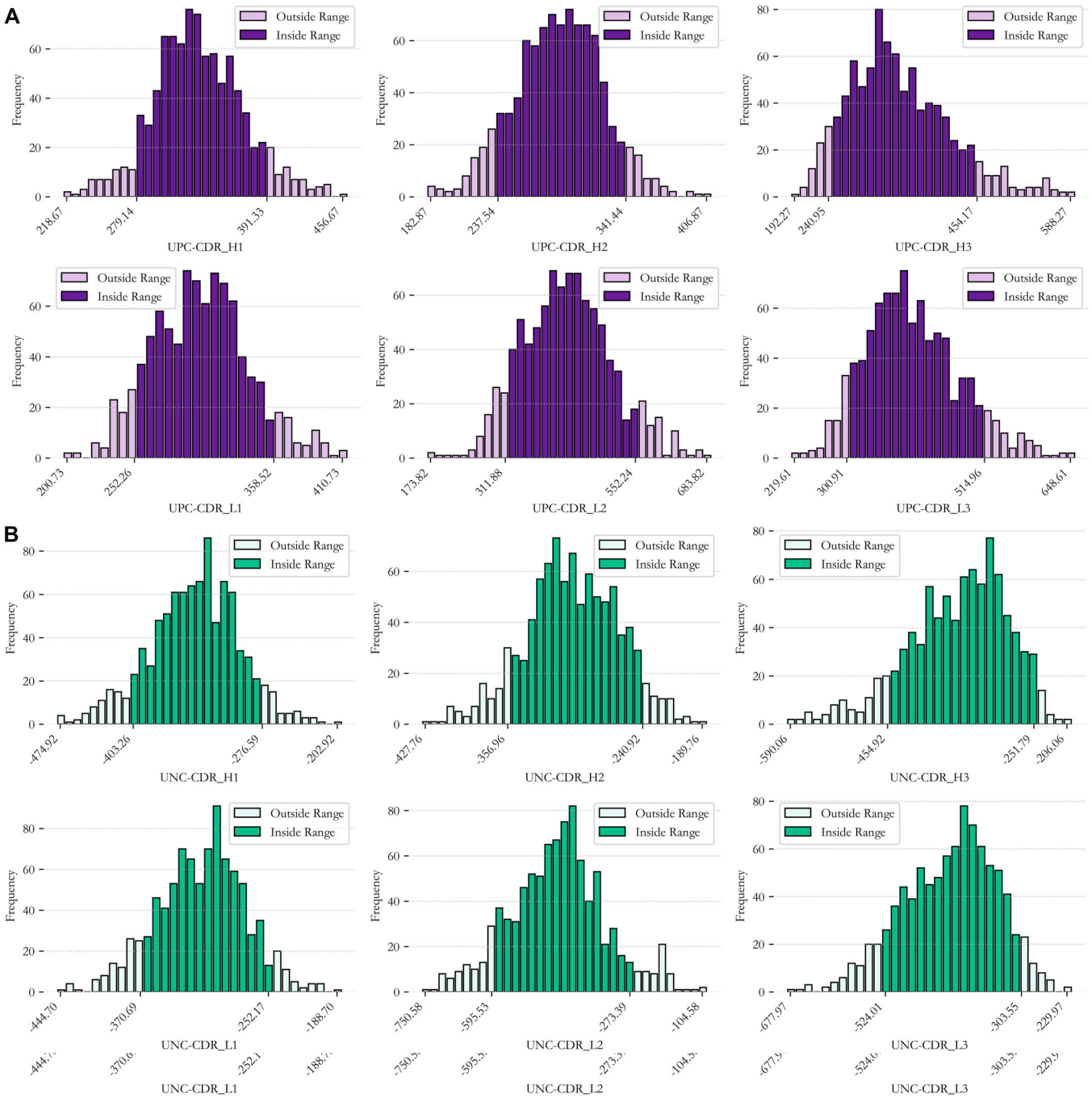

FIGURE 3 | The recommended range of UPC (A) and UNC (B) was constructed using 919 CST sequences. The purple and green bars represent the samples with charge distributions within the recommended range, whereas the gray bars indicate samples with charge distributions outside the recommended range.

Glembatumumab exhibits UPC CDR-H3 and UPC CDR-L1 values of 486.75 and 380.34, respectively, both of which significantly exceed the recommended thresholds. The distributions of UPC and UNC values for glembatumumab are visualized in Figure 4A,B.

Charge also impacts pharmacokinetic (PK) clearance, as the charge distribution in the variable fragment (Fv) of IgGs can lead to excessive FcRn binding, reducing FcRn-dependent terminal half-lives in vivo (Schoch et al. 2015). The antibody pair briakinumab and ustekinumab, with nearly identical IgG1 constant domains and similar isoelectric points, was used as a model system to investigate Fv charge distribution and PK clearance. Despite their similarities, briakinumab demonstrated a much shorter half-life than ustekinumab (Schoch et al. 2015). AB-Panda detected charge abnormalities in the CDR-L3 region of briakinumab, with a UPC value of 267.63 and a UNC value of −248.15, both exceeding the recommended thresholds. The UPC and UNC distribution of briakinumab is presented in Figure 4C,D. In contrast, AB-Panda detected no charge irregularities in ustekinumab. Meanwhile, TAP failed to identify any abnormalities in either antibody (Supporting Information Table S3).

3.3 | Interval Consistency Analysis: 919 CST Versus 166 Marketed

We also investigated whether the recommended range derived from 919 CST sequences (Table 1) could be validated using 166 antibody sequences approved for marketing (Supporting Information Table S4). As shown in Figure 5, The value

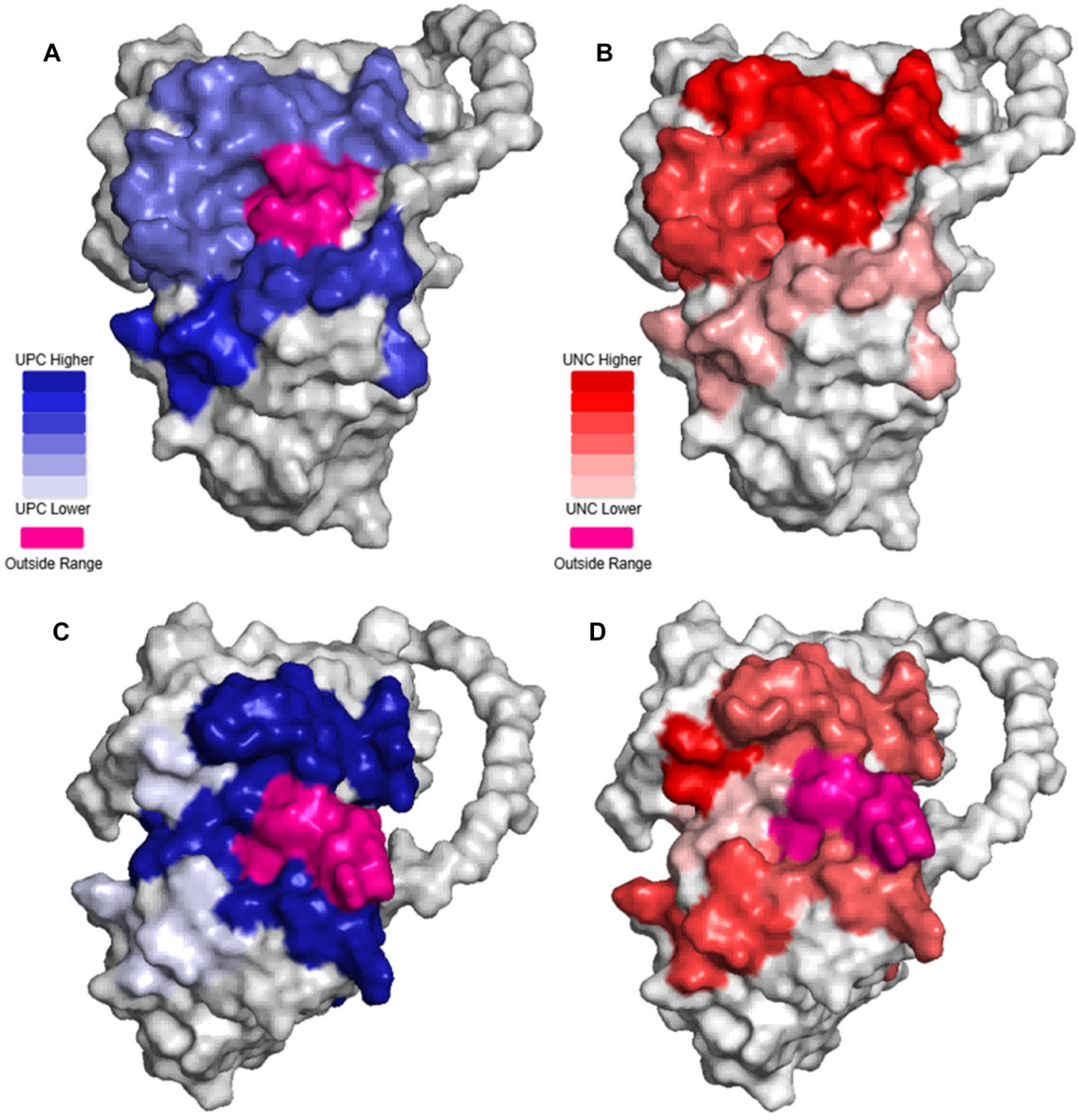

FIGURE 4 | The distribution of UPC and UNC across the CDRs of the antibody glembatumumab (A and B) and briakinumab (C and D). The intensity of the colors indicates the magnitude of UPC and UNC. Dark blue represents regions with higher UPC, while light blue indicates regions with lower UPC. Dark red signifies regions with higher UNC, whereas light red denotes regions with lower UNC. Hotpink represents areas outside the recommended range.

ranges established by AB-Panda for the 166 marketed sequences exhibit minimal differences compared to those of the 919 CST sequences. This suggests that the antibody developability profiler guidelines predicted by Panda, encompassing UHV, UPC, and UNC, align with the requirements for drug development in most cases. Further analysis, including paired t-tests and distribution comparisons between the two datasets, revealed no significant differences across the three metrics UHV, UPC, and UNC (p-values > 0.05). These statistical results indicate that the observed variations between the two datasets are likely due to random fluctuations rather than systematic bias. Furthermore, the box plot comparison shows a high degree of overlap in the distribution of UHV, UPC, and UNC between the two datasets, with the median values almost perfectly coinciding, indicating that the two datasets are very close in both central tendency and dispersion.

TABLE 1 | AB-Panda's recommended ranges of UHV, UPC and UNC based on data from 919 CSTs.

Metrics	Recommended ranges		
UHV-CDR_H1	−20.37	≤ UHV ≤	67.77
UHV-CDR_H2	−72.59	≤ UHV ≤	58.57
UHV-CDR_H3	−98.21	≤ UHV ≤	48.73
UHV-CDR_L1	−86.63	≤ UHV ≤	12.88
UHV-CDR_L2	−140.15	≤ UHV ≤	96.41
UHV-CDR_L3	−79.49	≤ UHV ≤	83.99
UPC-CDR_H1	279.14	≤ UPC ≤	391.33
UPC-CDR_H2	237.54	≤ UPC ≤	341.44
UPC-CDR_H3	240.95	≤ UPC ≤	454.17
UPC-CDR_L1	252.26	≤ UPC ≤	358.52
UPC-CDR_L2	311.88	≤ UPC ≤	522.24
UPC-CDR_L3	300.91	≤ UPC ≤	514.96
UNC-CDR_H1	−403.26	≤ UNC ≤	−276.59
UNC-CDR_H2	−356.96	≤ UNC ≤	−240.92
UNC-CDR_H3	−454.92	≤ UNC ≤	−251.79
UNC-CDR_L1	−370.69	≤ UNC ≤	−188.70
UNC-CDR_L2	−595.53	≤ UNC ≤	−273.39
UNC-CDR_L3	−524.01	≤ UNC ≤	−303.55

3.4 | AB-Panda Versus TAP

Among the 137 antibodies experimentally evaluated, we focused on those antibodies with two or more warning flags identified in biophysical assays, considering them potentially developability-challenged. These flagged antibodies were further analyzed using AB-Panda and TAP for comparative evaluation of their ability to detect developability issues (Supporting Information Table S2) (Jain 2017a). For the 14 approved antibody drugs with ≥ 2 warning flags, AB-Panda successfully identified 13 problematic cases, achieving a detection rate of 93%, whereas TAP identified only 1 case, with a detection rate of 7%. Similarly, among 18 antibodies in phase-3 trials, AB-Panda identified 13 problematic cases (detection rate: 72%), while TAP failed to detect any. For the 25 antibodies in phase-2 trials, AB-Panda identified 18 problematic cases (detection rate: 72%), significantly outperforming TAP, which detected 6 cases (detection rate: 24%).

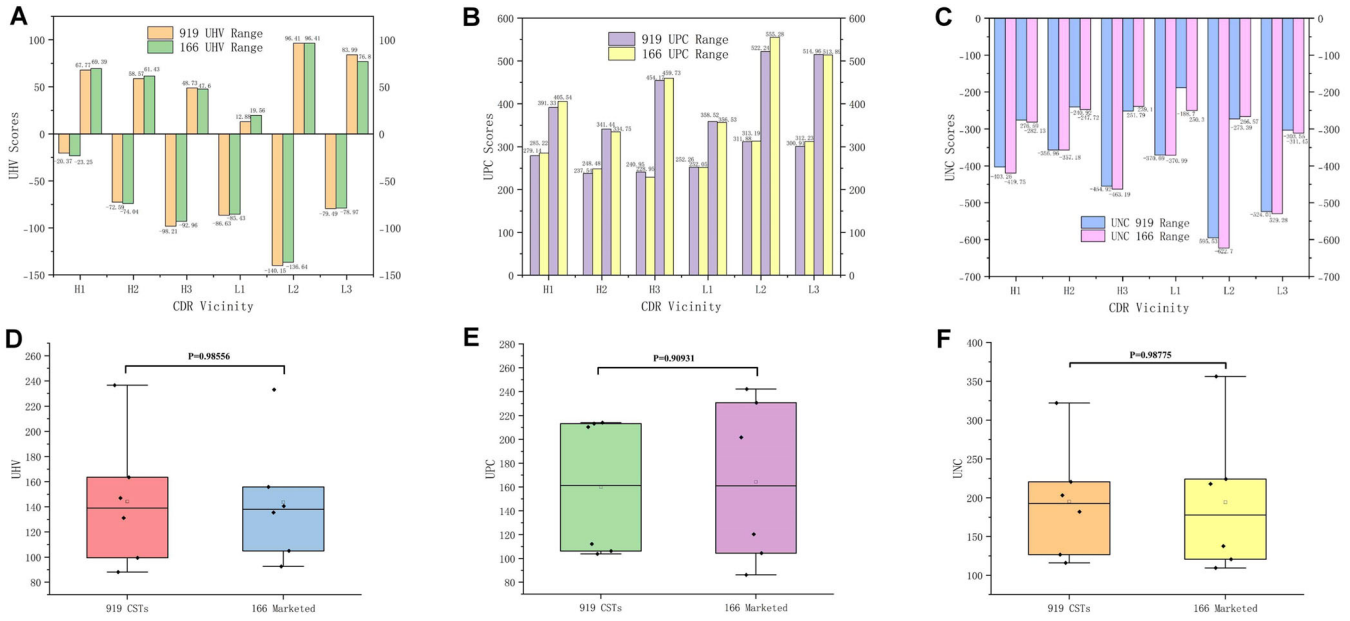

FIGURE 5 | Comparison of the recommended ranges for UHV (A), UPC (B), and UNC (C) between the 919 CST sequences and the 166 marketed sequences, where the x-axis represents the CDR regions (H1, H2, H3, L1, L2, L3) and the y-axis represents the corresponding UHV, UPC, or UNC values. (D), (E), and (F) show the differences in the length distributions of the three metrics (UHV, UPC, UNC) and present the statistical analysis comparing UHV, UPC, and UNC values between the 919 CST and the 166 marketed sequences. p-values > 0.05 indicate no significant differences between the datasets.

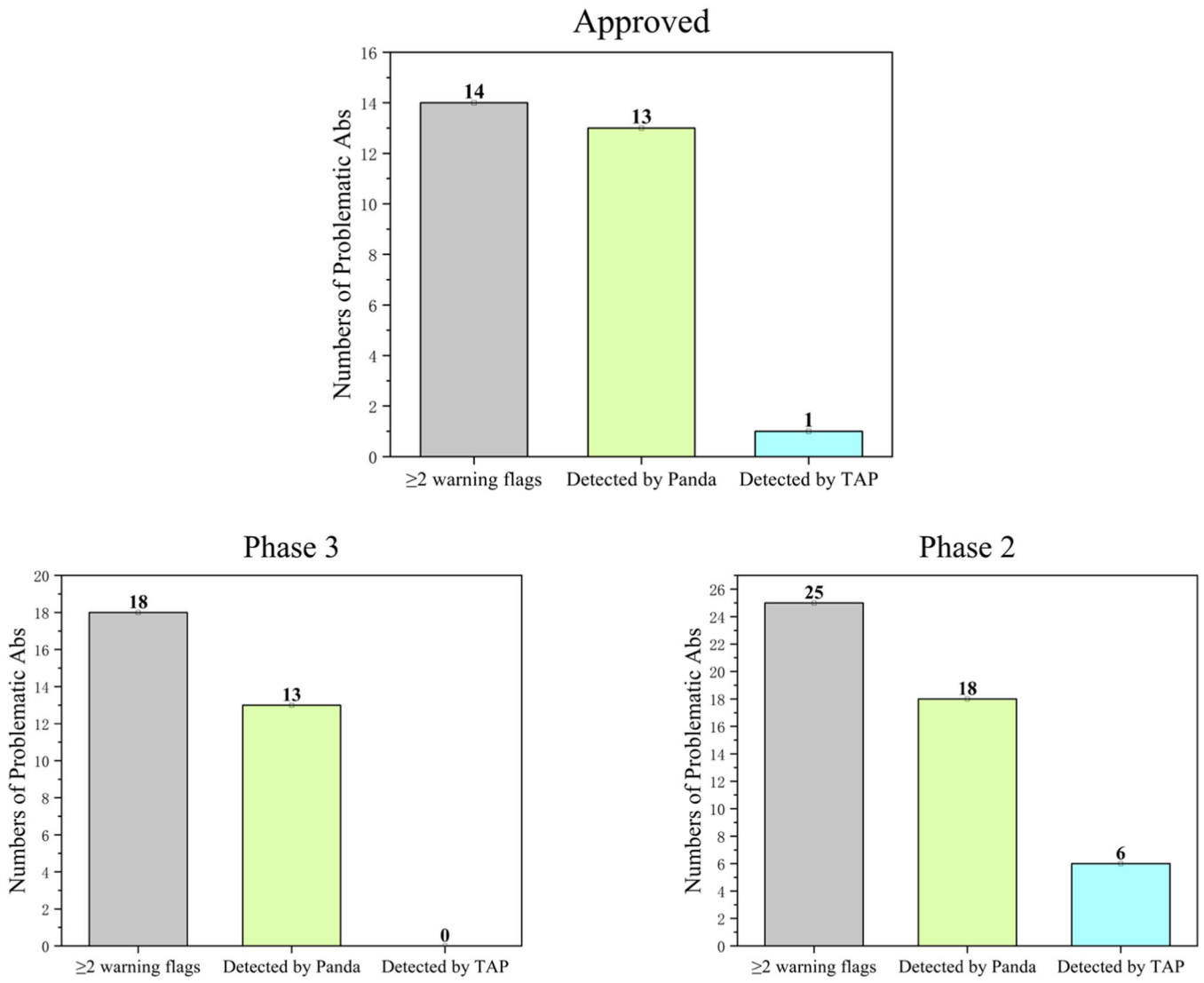

FIGURE 6 | Performance comparison of AB-Panda and TAP in predicting developability based on experimentally measured biophysical properties of antibodies across different clinical stages. Antibodies with two or more flags from biophysical experiments were classified as problematic and subsequently analyzed using AB-Panda or TAP. The histogram illustrates the number of problematic antibodies identified by AB-Panda versus TAP, highlighting AB-Panda's superior accuracy and effectiveness in detecting developability challenges.

These comparative results clearly demonstrate AB-Panda's superior performance in identifying developability-challenged antibodies across different development stages, reinforcing its value as a reliable tool in antibody screening and engineering (Figure 6). AB2 showed a slight advantage in predicting the structure of CDR-H1, CDR-H3, CDR-L1, and Framework-H regions, while AFM exhibited marginal superiority in CDR-H2, CDR-L2, CDR-L3, and Framework-L regions. Furthermore, AF2 outperforms AFM in monomeric structure predictionCurrently, AlphaFold2 (AF2) and ABodyBuilder2(AB2) are the best reliable tools for predicting antibody structure. To assesses whether different structure prediction model affects the accuracy of UHV, UPC, and UNC. We analyzed flagged antibodies among the 137 antibodies using UHV, UPC, and UNC values derived from structures generated by either AF2 or AB2. As illustrated in Figure S7, AF2 identified 44 problematic antibodies, while AB2 also detected 44 problematic antibodies, with only slightly differences in the specific antibodies flagged by the two models. These results suggested that different structure model would not significantly impact the performance of AB-Panda.

4 | Discussion

In this study, we introduced AB-Panda, a structure-based antibody computation tool for developability prediction. AB-Panda incorporates three innovative metrics—UHV, UPC, and UNC—and integrates them with 3D visualization software to deliver detailed, intuitive insights into surface hydrophobicity and charge distribution. This approach enables researchers to pinpoint critical regions within the antibody structure and make informed decisions for sequence optimization.

Surface patches of positive and negative charges in the CDR regions have been shown to adversely affect viscosity and pharmacokinetics, while modifying the charge patches often result in

significant pharmacokinetic improvement (Chen et al. 2024; Sun et al. 2020; Datta-Mannan et al. 2015). Similarly, surface hydrophobicity is critical for predicting developability, as it is closely related to molecular aggregation risk and stability (Yuan et al. 2023). Excessive hydrophobicity may lead to nonspecific binding of antibodies, increasing the risk of interactions with off-target molecules and potentially causing side effects (Tang et al. 2018). In contrast, optimal distribution of hydrophobicity can enhance antibody stability under physiological conditions, improving its therapeutic potential (Geller et al. 2018b).

The hydrophobicity and charge interactions of antibodies are primarily determined by the surface-exposed amino acids, particularly those within the CDRs (Jain 2017b; Visalakshan et al. 2019). Advanced AI-driven structural prediction tools are crucial for accurately modeling the spatial distribution of these surface amino acids. In a recent benchmarking study involving 34 antibodies with experimentally solved structures, AB2 and Alphafold2-Multimer (AFM) demonstrated comparable overall accuracy. AB2 showed a slight advantage in predicting the structure of CDR-H1, CDR-H3, CDR-L1, and Framework-H regions, while AFM exhibited marginal superiority in CDR-H2, CDR-L2, CDR-L3, and Framework-L regions. Since the standard AlphaFold2 (AF2) is known to outperform AFM for monomeric structures, we connected the VH and VL domains using a 3xG4S linker. Subsequent molecular docking and dynamics simulations confirmed that this linker mimics the native antibody structure without disrupting antigen binding (Figures S1–S6, Table S5) (Jumper et al. 2021; A Abanades et al. 2023), Moreover, we tested whether the choice of structure prediction model (AF2 or AB2) affects the accuracy of UHV, UPC, and UNC metrics. Among 137 experimentally evaluated antibodies, both models identified 44 problematic antibodies with slight differences in specific cases (Figure S7). Based on the data and existing literature, we conclude that the use of either AF2 or AB2 has no significant impact on Panda's performance.

AB-Panda goes beyond structural precision by focusing on detailed, localized characterization of hydrophobicity and charge patterns within individual CDR loops. Unlike TAP, which evaluates overall charge and hydrophobicity across the entire antibody structure, AB-Panda highlights local variations, enabling precise identification of problematic CDR regions and specific amino acid residues for optimization. This level of granularity provides researchers with actionable insights for targeted modifications to improve antibody performance. In a systematic comparison with TAP, AB-Panda consistently outperformed it in predicting developability based on experimentally measured biophysical and pharmacokinetic (PK) properties, as shown in Figures 2, 4, and 5. By mapping critical physicochemical features across all six CDRs, AB-Panda offers a robust framework for identifying mutation sites and designing informed sequence modifications.

By combining UHV with UPC and UNC, we have established a comprehensive set of metrics to assess antibody developability. The recommended value ranges presented in Table 1 provide standardized reference points for hydrophobicity and charge distribution across each CDR region. A comparison of these ranges from 919 CST antibodies with values from 166 approved antibodies revealed no significant differences (Figure 6). However, some antibodies fall outside the recommended ranges yet have successfully advanced through development. For example, Alirocumab, an antibody approved for the treatment of hypercholesterolemia and administered subcutaneously at concentrations of 75 or 150 mg/ml, has a CDRH1 UHV score of −74.2445 as predicted by AB-Panda, which lies outside the established range. This discrepancy might be partially attributed to the limited sample size, which may reduce the statistical power and slightly affect AB-Panda's prediction accuracy. Thus, ongoing integration of new experimental data is critical to refining the UHV, UPC, and UNC reference ranges for improved accuracy.

On our website, we have also incorporated previously established parameters associated with antibody developability, including the total length of antibody CDRs, the isoelectric point of antibody Fv (FV PI), charge separation between the light and heavy chains of the Fv (FV CSP), and the high viscosity index of antibody (FV HVI). It is crucial to stress that antibody developability is influenced not only by intrinsic molecular properties of antibodies, but also by external physicochemical factors, such as temperature, pH, and storage conditions (Streich and Lima 2016; Oliva et al. 2020). These external factors can significantly impact antibody stability during later stages of drug development, ultimately affecting their clinical application. Therefore, localized analyzes focusing on specific regions, such as CDR H1-H3 or CDR L1-L3, can be conducted by integrating experimental conditions to explore potential regional variations in antibody behavior.

Utilizing AI-generated antibody structures and three innovative metrics, AB-Panda empowers researchers to identify and address developability issues in specific antibody regions, enabling more targeted and efficient optimization. Future developments will incorporate antibody sequences from recent clinical trials and further refine AB-Panda based on laboratory data feedback.

Author Contributions

Wu Zou conceptualized the research idea, led the data analysis, wrote the main manuscript content, contributed to the creation of all figures and tables, and facilitated the clear presentation of research data and findings. Jianjun Deng compiled and analyzed all data, developed the website, and contributed to the discussion of the methodology details. Yun Shen provided technical guidance and participated in the website development. Tao Zhang participated in work discussions, reviewed, edited, and supervised the article. Zhitong Bing assisted in the final revision of the article. Lingyan Yuan conducted formal analysis, investigation, and manuscript review. Jianghai Liu conceptualized the study, designed the experimental plan, and defined the experimental objectives and research themes. XinLei Li reviewed, edited, revised, and supervised, participated in the methodology discussion, provided ideas for figure creation, and assisted in the final article revision.

Conflicts of Interest

The authors declare no conflicts of interest.

Data Availability Statement

All data generated or analyzed during this study are included in this published article and its supplementary information files.

References

Abanades, B., W. K. Wong, F. Boyles, G. Georges, A. Bujotzek, and C. M. Deane. 2023. "Immunebuilder: Deep-Learning Models for Predicting the Structures of Immune Proteins." *Communications Biology* 6: 575.

Bailly, M., C. Mieczkowski, V. Juan, et al. 2020. "Predicting Antibody Developability Profiles Through Early Stage Discovery Screening." *mAbs* 12: 1743053.

Calvo, B., and L. Zuniga. 2012. "Therapeutic Monoclonal Antibodies: Strategies and Challenges for Biosimilars Development." *Current Medicinal Chemistry* 19: 4445–4450.

Chen, H. T., Y. Zhang, J. Huang, et al. 2024. "Human Antibody Polyreactivity is Governed Primarily by the Heavy-Chain Complementarity-Determining Regions." *Cell Reports* 43: 114801.

Cock, P. J. A., T. Antao, J. T. Chang, et al. 2009. "Biopython: Freely Available Python Tools for Computational Molecular Biology and Bioinformatics." *Bioinformatics* 25: 1422–1423.

Condado-Morales, I., F. Dingfelder, I. Waibel, et al. 2024. "A Comparative Study of the Developability of Full-Length Antibodies, Fragments, and Bispecific Formats Reveals Higher Stability Risks for Engineered Constructs." *mAbs* 16: 2403156.

Datta-Mannan, A., A. Thangaraju, D. Leung, et al. 2015. "Balancing Charge In the Complementarity-Determining Regions of Humanized Mabs Without Affecting pI Reduces Non-Specific Binding and Improves the Pharmacokinetics." *mAbs* 7: 483–493.

DiMasi, J. A., H. G. Grabowski, and R. W. Hansen. 2016. "Innovation In the Pharmaceutical Industry: New Estimates of R&D Costs." *Journal of Health Economics* 47: 20–33.

Eisenberg, D., E. Schwarz, M. Komaromy, and R. Wall. 1984. "Analysis of Membrane and Surface Protein Sequences With the Hydrophobic Moment Plot." *Journal of Molecular Biology* 179: 125–142.

Fazenda, M. L., J. M. Dias, L. M. Harvey, et al. 2013. "Towards Better Understanding of an Industrial Cell Factory: Investigating the Feasibility of Real-Time Metabolic Flux Analysis in Pichia Pastoris." *Microbial Cell Factories* 12: 51.

Fogel, D. B. 2018. "Factors Associated With Clinical Trials That Fail and Opportunities for Improving the Likelihood of Success: A Review." *Contemporary Clinical Trials Communications* 11: 156–164.

Fugger, L., L. T. Jensen, and J. Rossjohn. 2020. "Challenges, Progress, and Prospects of Developing Therapies to Treat Autoimmune Diseases." *Cell* 181: 63–80.

Geller, R., S. Pechmann, A. Acevedo, R. Andino, and J. Frydman. 2018a. "Hsp90 Shapes Protein and RNA Evolution to Balance Trade-Offs Between Protein Stability and Aggregation." *Nature Communications* 9: 1781.

Geller, R., S. Pechmann, A. Acevedo, R. Andino, and J. Frydman. 2018b. "Hsp90 Shapes Protein and RNA Evolution to Balance Trade-Offs Between Protein Stability and Aggregation." *Nature Communications* 9: 1781.

Hebditch, M., and J. Warwicker. 2019. "Web-Based Display of Protein Surface and pH-Dependent Properties for Assessing the Developability of Biotherapeutics." *Scientific Reports* 9: 1969.

Hladílková, J., T. H. Callisen, and M. Lund. 2016. "Lateral Protein-Protein Interactions at Hydrophobic and Charged Surfaces as a Function of pH and Salt Concentration." *The Journal of Physical Chemistry B* 120: 3303–3310.

Jain, T., T. Sun, S. Durand, et al. 2017a. "Biophysical Properties of the Clinical-Stage Antibody Landscape." *Proceedings of the National Academy of Sciences of the United States of America* 114: 944–949.

Jain, T., T. Boland, A. Lilov, et al. 2017b. "Prediction of Delayed Retention of Antibodies in Hydrophobic Interaction Chromatography From Sequence Using Machine Learning." *Bioinformatics* 33: 3758–3766.

Jiskoot, W., A. Hawe, T. Menzen, D. B. Volkin, and D. J. A. Crommelin. 2022. "Ongoing Challenges to Develop High Concentration Monoclonal Antibody-Based Formulations for Subcutaneous Administration: Quo Vadis?" *Journal of Pharmaceutical Sciences* 111: 861–867.

Jumper, J., R. Evans, A. Pritzel, et al. 2021. "Highly Accurate Protein Structure Prediction With Alphafold." *Nature* 596: 583–589.

Li, J., Y. Cheng, X. Chen, and S. Zheng. 2019. "Impact of Electroviscous Effect on Viscosity in Developing Highly Concentrated Protein Formulations: Lessons From Non-Protein Charged Colloids." *International Journal of Pharmaceutics: X* 1: 100002.

Liu, J., M. D. H. Nguyen, J. D. Andya, and S. J. Shire. 2005. "Reversible Self-Association Increases the Viscosity of a Concentrated Monoclonal Antibody in Aqueous Solution." *Journal of Pharmaceutical Sciences* 94: 1928–1940.

Oliva, R., S. Banerjee, H. Cinar, C. Ehrt, and R. Winter. 2020. "Alteration of Protein Binding Affinities by Aqueous Two-Phase Systems Revealed by Pressure Perturbation." *Scientific Reports* 10: 8074.

Pleguezuelo, D. E., R. Díaz-Simón, O. Cabrera-Marante, et al. 2021. "Case Report: Resetting the Humoral Immune Response by Targeting Plasma Cells With Daratumumab in Anti-Phospholipid Syndrome." *Frontiers in Immunology* 12: 667515.

Raybould, M. I. J., C. Marks, K. Krawczyk, et al. 2019. "Five Computational Developability Guidelines for Therapeutic Antibody Profiling." *Proceedings of the National Academy of Sciences* 116: 4025–4030.

Raybould, M. I. J., O. M. Turnbull, A. Suter, B. Guloglu, and C. M. Deane. 2024. "Contextualising the Developability Risk of Antibodies With Lambda Light Chains Using Enhanced Therapeutic Antibody Profiling." *Communications Biology* 7: 62.

Schoch, A., H. Kettenberger, O. Mundigl, et al. 2015. "Charge-Mediated Influence of the Antibody Variable Domain on FcRN-Dependent Pharmacokinetics." *Proceedings of the National Academy of Sciences* 112: 5997–6002.

Song, Y., H. Jeong, S. R. Kim, et al. 2021. "Dissecting the Impact of Target-Binding Kinetics of Protein Binders on Tumor Localization." *iScience* 24: 102104.

Sripriya Akondi, V., V. Menon, J. Baudry, and J. Whittle. 2022. "Novel Big Data-Driven Machine Learning Models for Drug Discovery Application." *Molecules* 27: 594.

Streich, Jr., F. C., and C. D. Lima. 2016. "Capturing a Substrate in an Activated Ring E3/E2-SUMO Complex." *Nature* 536: 304–308.

Sun, Y., H. Cai, Z. Hu, et al. 2020. "Balancing the Affinity and Pharmacokinetics of Antibodies by Modulating the Size of Charge Patches on Complementarity-Determining Regions." *Journal of Pharmaceutical Sciences* 109: 3690–3696.

Tang, Y. H., H. C. Lin, C. L. Lai, P. Y. Chen, and C. H. Lai. 2018. "Mannosyl Electrochemical Impedance Cytosensor for Label-Free MDA-MB-231 Cancer Cell Detection." *Biosensors and Bioelectronics* 116: 100–107.

Thorsteinson, N., J. R. Gunn, K. Kelly, W. Long, and P. Labute. 2021. "Structure-Based Charge Calculations for Predicting Isoelectric Point, Viscosity, Clearance, and Profiling Antibody Therapeutics." *mAbs* 13: 1981805.

Tien, M. Z., A. G. Meyer, D. K. Sydykova, S. J. Spielman, and C. O. Wilke. 2013. "Maximum Allowed Solvent Accessibilites of Residues in Proteins." *PLoS One* 8: e80635.

Visalakshan, R. M., M. N. MacGregor, S. Sasidharan, et al. 2019. "Biomaterial Surface Hydrophobicity-Mediated Serum Protein Adsorption and Immune Responses." *ACS Applied Materials and Interfaces* 11: 27615–27623.

Wang, W., S. Nema, and D. Teagarden. 2010. "Protein Aggregation--Pathways and Influencing Factors." *International Journal of Pharmaceutics* 390: 89–99.

Yamankurt, G., E. J. Berns, A. Xue, et al. 2019. "Exploration of the Nanomedicine-Design Space With High-Throughput Screening and Machine Learning." *Nature Biomedical Engineering* 3: 318–327.

Yuan, Z., P. McMullen, S. Luozhong, et al. 2023. "Hidden Hydrophobicity Impacts Polymer Immunogenicity." *Chemical Science* 14: 2033–2039.

Supporting Information

Additional supporting information can be found online in the Supporting Information section.
receptor-ligand. Supplement Tables. Supplementary Files.